Effects of non-conserved magnetization operator on the magneto-thermal properties of spin clusters and chains.

Vadim Ohanyan

Laboratory of Theoretical Physics
Yerevan State University
&
CANDLE SRI

Yerevan, 16 May 2019

- Jozef Strečka, *P.J. Šafárik University, Košice, Slovakia*
- Onofre Rojas, *Universidade Federal de Lavras, Lavras, Brazil*
- Jordana Torrico, *Universidade Federal de Alagoas, Maceió, Brazil*
- Stefano Bellucci, *LNF INFN, Frascati, Italy*
- Oleg Derzhko, Taras Krokhmalskii, Taras Verkholyak, Ostap Baran, *ICMP, Lviv, Ukraine*

- S. Bellucci and V. O., and O. Rojas, Magnetization non-rational quasi-plateau and spatially modulated spin order in the model of the single-chain magnet, $[\{(CuL)_2Dy\}\{Mo(CN)_8\}] \cdot 2CH_3CN \cdot H_2O$, EPL **105**, 47012 (2014).
- V. O., O. Rojas, J. Strečka, and S. Bellucci, Absence of actual plateaus in zero-temperature magnetization curves of quantum spin clusters and chains, Phys. Rev. B **92**, 214423 (2015).
- J. Torrico, V. O., and O. Rojas, Non-conserved magnetization operator and 'fire-and-ice' ground states in the Ising-Heisenberg diamond chain, J. Magn. Magn. Mater. **454**, 85 (2018).
- T. Ktokhmalskii, T. Verkholyak, O. Baran, V. O., O. Derzhko, Spin-1/2 XX chain in a transverse field with regularly alternating g-factors, (in progress)

- Few-body vs. Many-body spin systems
- Non-conserving magnetization
  - S=1/2 spin dimer
  - S=1-1/2 mixed spin dimer
  - S=1/2 spin trimer (triangle)
- Coordination polymer $[\{(CuL)_2Dy\}\{Mo(CN)_8\}] \cdot 2CH_3CN \cdot H_2O$
  - The model and parameters from the experimental data and fitting.
  - Exact solution
  - Eigenstates and magnetization
  - Quasi-plateau

- negative g-factros
  - "fire-and-ice" ground states, Ising chain
  - "fire-and-ice" ground states, Ising diamond chain
- Ising-Heisenberg diamond chain with different g-factors
  - eigenvalues and eigenstates
  - phase diagrams
  - "fire-and-ice" ground states
- XX-chain with the staggered g-factros
  - diagonalization of the Hamiltonian
  - g-factors with different signs
  - effect of staggered and negative g-factors on the dynamical structure factros

FEW-BODY VS. MANY-BODY SPIN SYSTEMS

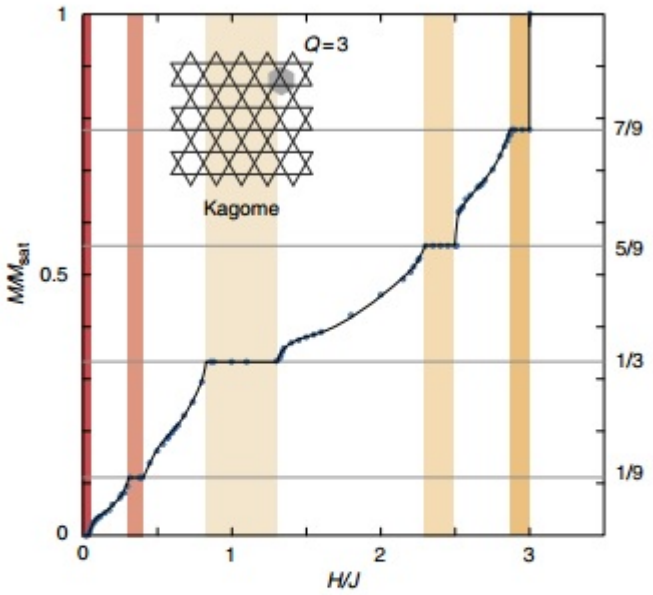

| Magnetization curve of the spin-1/2 kagome Heisenberg antiferromagnet in a uniform magnetic field. The saturation value of the magnetization density per site is $M_{sat}/N = 1/2$. The inset shows the geometry of the kagome lattice. The shaded hexagon is the original lattice unit cell including three sites ($Q = 3$). Data points are obtained by the grand canonical analysis on a hexagonal cluster with $N = 114$ and 132, which directly gives the curve of the thermodynamic limit without any size scaling. The range of each plateau is highlighted.

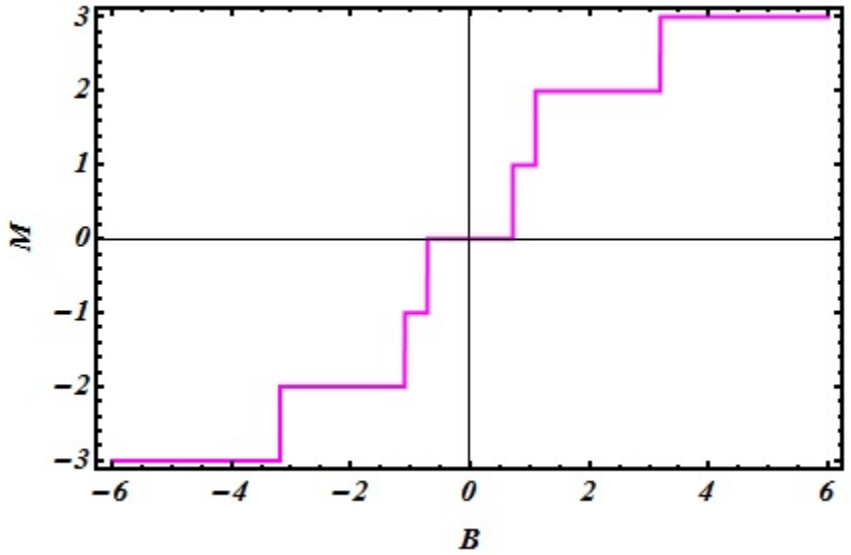

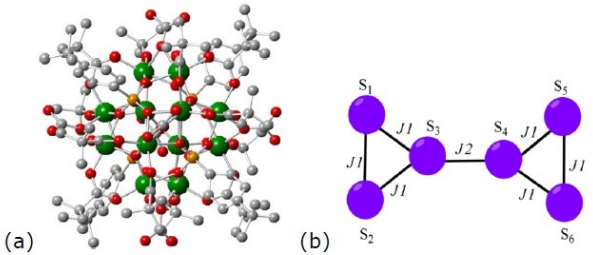

Molecular structure of $[Ni_{12}(\mu_3\text{-}OH)_4(HCO_3)_6(O_3PR)_4(O_2C^tBu)_6\ (HO_2CtBu)_6]$ (R = p-tert-Butylphenyl) in the crystal (a) and its theoretical model (b).

S. Nishimori, N. Shibata, C. Hotta, Nature Comm. 4, 2287 (2013)

MAGNETIZATION IN VARIOUS SYSTEMS

SPIN CLUSTERS. MOLECULAR MAGNETS

$$\mathcal{M}^z = g\mu_B \sum_{i=1}^{N} S_i^z, \qquad [H, \mathcal{M}^z] = 0$$

$$H = H_0 - B\mathcal{M}^z, \;\; \Rightarrow \;\; E_n = E_n(0) - m_n B$$

$$H_0|\Psi_n\rangle = E_n(0)|\Psi_n\rangle$$

$$\mathcal{M}_z|\Psi_n\rangle = m_n|\Psi_n\rangle$$

ALL EIGENVALUES ARE LINEAR IN MAGNETIC FIELD

EACH EIGENSTATE HAS FIXED CONSTANT MAGNETIC MOMENT

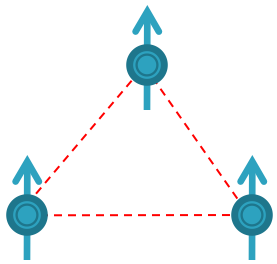

S=1

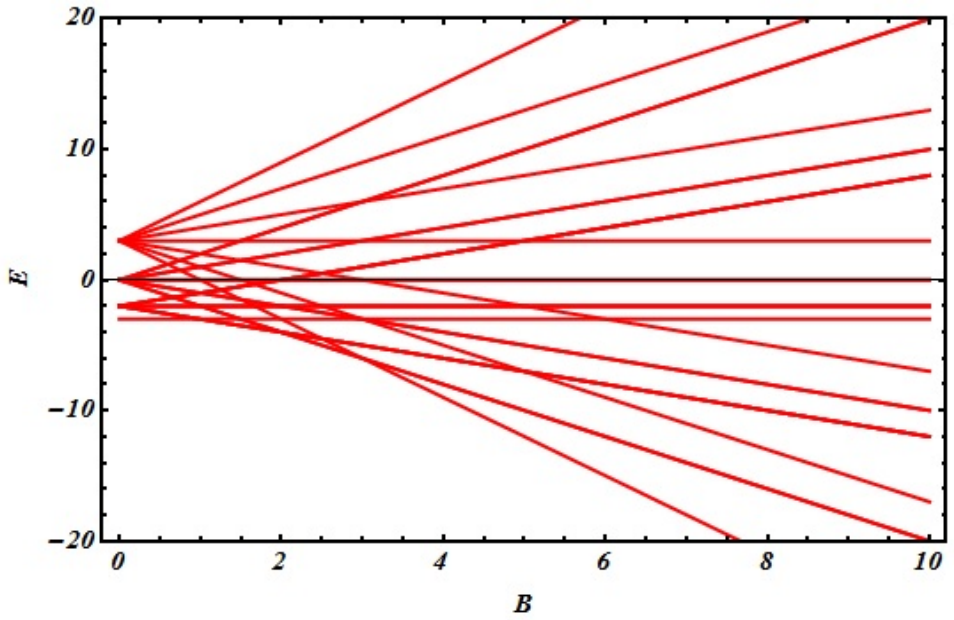

NON-CONSERVING MAGNETIZATION

$$[\mathcal{H}, \mathcal{M}^z] \neq 0.$$

$$[\mathcal{H}, S^z_{\rm tot}] \neq 0, \quad \mathcal{M}^z = g\mu_B S^z_{\rm tot}$$

$$[\mathcal{H}, S^z_{\rm tot}] = 0, \quad \mathcal{M}^z \neq g\mu_B S^z_{\rm tot}$$

SPIN-1/2 HEISENBERG DIMER

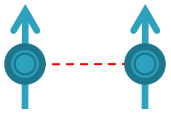

$$\mathcal{H} = J\left\{(1+\gamma)\, S_1^x S_2^x + (1-\gamma)\, S_1^y S_2^y + \Delta S_1^z S_2^z\right\} + \mathbf{D}\cdot(\mathbf{S}_1 \times \mathbf{S}_2) - \mathbf{B}\,(g_1 \boldsymbol{S}_1 + g_2 \boldsymbol{S}_2)$$

$$\mathbf{B} = (0, 0, B), \quad \mathbf{D} = (D_x, 0, D_z)$$

$$\mathcal{H} = J\left\{(1+\gamma)\, S_1^x S_2^x + (1-\gamma)\, S_1^y S_2^y + \Delta S_1^z S_2^z\right\} + D_x\,(S_1^y S_2^z - S_1^z S_2^y) + D_z\,(S_1^x S_2^y - S_1^y S_2^x) - B\,(g_1 S_1^z + g_2 S_2^z).$$

$$S^z_{tot} = S^z_1 + S^z_2, \quad \mathcal{M}^z = g_1 S^z_1 + g_2 S^z_2,$$

NON-CONSERVING MAGNETIZATION

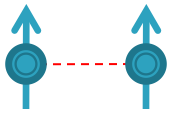

SPIN-1/2 HEISENBERG DIMER

$$[\mathcal{H},\ S^z] = -2i\gamma\,(S_1^x S_2^y + S_1^y S_2^x) + iD_x\,(S_1^x S_2^z - S_1^z S_2^x)$$

$$[\mathcal{H},\ \mathcal{M}^z] = i(g_2 - g_1)\,\{D_z\,(S_1^x S_2^x + S_1^y S_2^y) - J\,(S_1^x S_2^y - S_1^y S_2^x)\} - i\gamma(g_1 + g_2)\,(S_1^x S_2^y + S_1^y S_2^x) + iD_x\,(g_1 S_1^x S_2^z - g_2 S_1^z S_2^x)$$

$$\varepsilon_{1,2} = -\frac{J\Delta}{4} \pm \frac{1}{2}\sqrt{B^2 g_-^2 + J^2 + D_z^2}$$

$$\varepsilon_{3,4} = \frac{J\Delta}{4} \pm \frac{1}{2}\sqrt{B^2 g_+^2 + J^2\gamma^2}$$

$$|\Psi_{1,2}\rangle = \frac{1}{\sqrt{1+|A_\pm|^2}}(|\uparrow\downarrow\rangle + A_\pm|\downarrow\uparrow\rangle),$$

$$A_\pm = \rho_\pm e^{i\phi}, \quad \phi = \arctan\frac{D_z}{J},$$

$$\rho_\pm = \frac{Bg_- \pm \sqrt{B^2 g_-^2 + J^2 + D_z^2}}{\sqrt{J^2 + D_z^2}},$$

$$|\Psi_{3,4}\rangle = \frac{1}{\sqrt{1+B_\pm^2}}(|\uparrow\uparrow\rangle + B_\pm|\downarrow\downarrow\rangle),$$

$$B_\pm = \frac{Bg_+ \pm \sqrt{B^2 g_+^2 + J^2\gamma^2}}{J\gamma}.$$

$$m_{1,2} = \langle\Psi_{1,2}|\,(g_1 S_1^z + g_2 S_2^z)\,|\Psi_{1,2}\rangle = \pm\frac{B(g_1 - g_2)^2}{2\sqrt{B^2(g_1 - g_2)^2 + J^2 + D_z^2}}$$

$$m_{3,4} = \langle\Psi_{3,4}|\,(g_1 S_1^z + g_2 S_2^z)\,|\Psi_{3,4}\rangle = \pm\frac{B(g_1 + g_2)^2}{2\sqrt{B^2(g_1 + g_2)^2 + J^2\gamma^2}}$$

NON-CONSERVING MAGNETIZATION

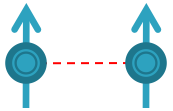

SPIN-1/2 HEISENBERG DIMER

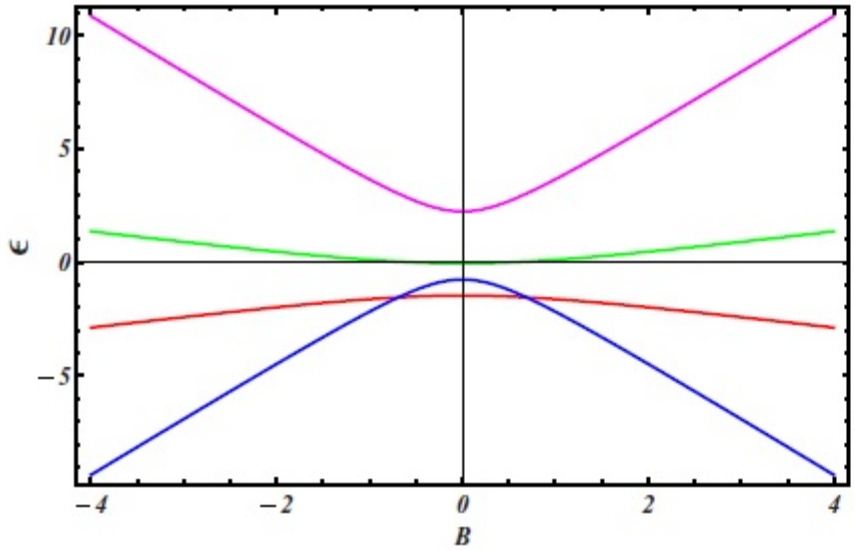

The energy spectrum of the isolated $S = 1/2$ dimer with $g_1 = 2$, $g_2 = 3$, $J = 1$, $D_z = 1$, $\gamma = 2$, and $\Delta = 3$ displaying level crossing. The two bottom curves correspond to ε_2 and ε_4. The nonlinearity in B on the energy levels is the main reason for the nonplateau magnetization.

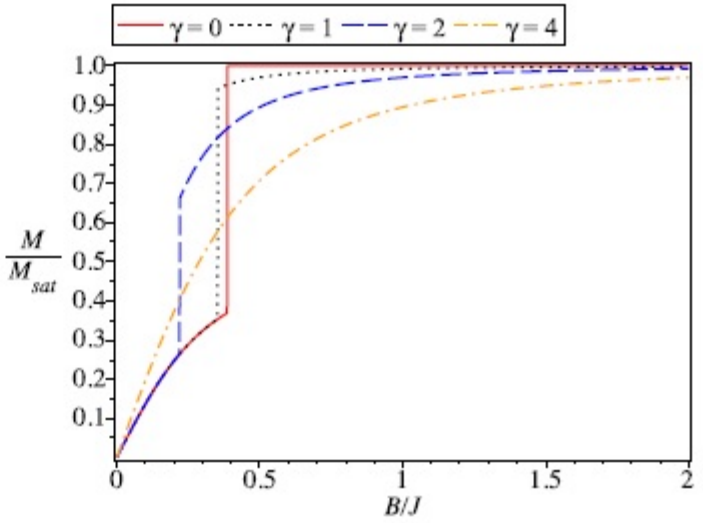

The zero-temperature magnetization curves for the $S = 1/2$ dimer with $g_1 = 2$, $g_2 = 6$, $J = 1$, $D_z = 1$, $\Delta = 2$, and $\gamma = 0$ (red, solid); $\gamma = 1$ (black, dotted); $\gamma = 2$ (blue, dashed); and $\gamma = 4$ (orange, dot-dashed). $M_{\text{sat}} = \frac{1}{2}(g_1 + g_2) = 4$.

NON-CONSERVING MAGNETIZATION

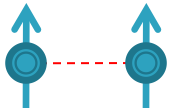

SPIN-1/2 HEISENBERG DIMER

$$B_c = J\frac{g_+\Delta + \sqrt{g_-^2\Delta^2 + 4g_1g_2}}{4g_1g_2}.$$

Thus, the jump to the saturated magnetization takes place for $\gamma = 0$ at this value of the magnetic field. The magnitude of the jump depends on the difference of the Landé g factors and is given by

$$\Delta M = \frac{g_+}{2}\left\{1 - \frac{g_-^2\left[\Delta + \frac{\sqrt{g_-^2\Delta^2+4g_1g_2}}{g_+}\right]}{4g_1g_2\sqrt{1+\frac{g_-^2[g_+\Delta+\sqrt{g_-^2\Delta^2+4g_1g_2}]}{16g_1^2g_2^2}}}\right\}$$

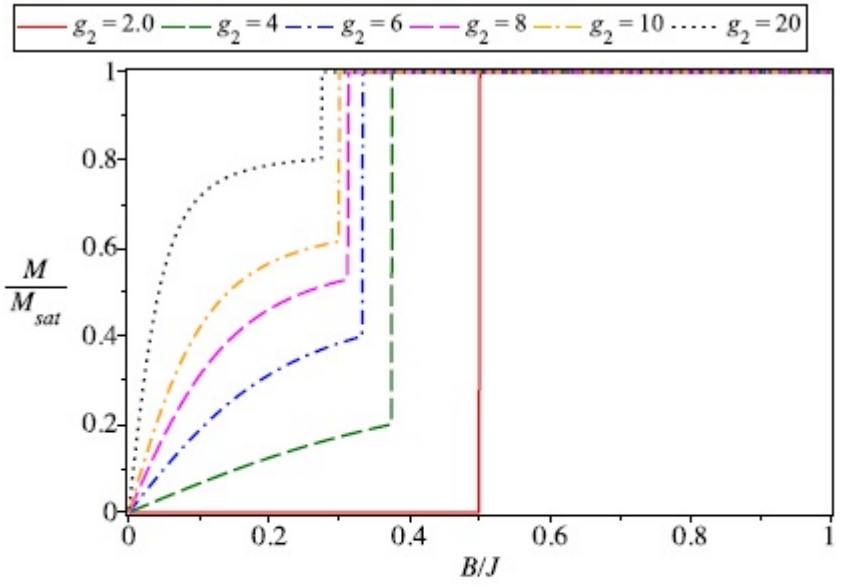

FIG. 3. (Color online) The normalized zero-temperature magnetization curves $M/M_{\rm sat}$ of the $S = 1/2$ dimer with two different g factors in case of isotropic exchange interaction, $\gamma = 0$ and $\Delta = 1$. Here, for the sake of simplicity, we put $J = 1, D_z = 0, g_1 = 2$ and present the curves for the different values of g_2. From the bottom to top $g_2 = 2$ (red); 4 (green); 6 (blue); 8 (magenta); 10 (orange); and 20 (black). $M_{\rm sat} = \frac{1}{2}(g_1 + g_2)$.

NON-CONSERVING MAGNETIZATION

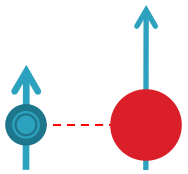

MIXED SPIN-(1/2,1) HEISENBERG DIMER

$$\mathcal{H}_{1/2-1} = J\left(S_1^x\mu_2^x + S_1^y\mu_2^y + \Delta S_1^z\mu_2^z\right) + D(\mu_2^z)^2 - B(g_1 S_1^z - g_2\mu_2^z.)$$

$$\varepsilon_{1,2} = \frac{1}{2}J\Delta + D \mp \frac{B}{2}(g_1 + 2g_2),$$

$$\varepsilon_{3,4} = -\frac{1}{4}(J\Delta - 2D + 2g_2B) \mp \frac{1}{4}\sqrt{(J\Delta - 2D - 2g_-B)^2 + 8J^2},$$

$$\varepsilon_{5,6} = -\frac{1}{4}(J\Delta - 2D - 2g_2B) \mp \frac{1}{4}\sqrt{(J\Delta - 2D + 2g_-B)^2 + 8J^2},$$

$$|\Psi_{1,2}\rangle = \left|\mp\tfrac{1}{2}, \mp 1\right\rangle,$$

$$|\Psi_{3,4}\rangle = c_1^{\pm}\left|-\tfrac{1}{2}, 1\right\rangle \mp c_1^{\mp}\left|\tfrac{1}{2}, 0\right\rangle,$$

$$|\Psi_{5,6}\rangle = c_2^{\pm}\left|\tfrac{1}{2}, -1\right\rangle \mp c_2^{\mp}\left|-\tfrac{1}{2}, 0\right\rangle,$$

where the respective probability amplitudes are given by

$$c_1^{\pm} = \sqrt{\frac{1}{2}\left[1 \pm \frac{J\Delta - 2D - 2g_-B}{\sqrt{(J\Delta - 2D - 2g_-B)^2 + 8J^2}}\right]},$$

$$c_2^{\pm} = \sqrt{\frac{1}{2}\left[1 \pm \frac{J\Delta - 2D + 2g_-B}{\sqrt{(J\Delta - 2D + 2g_-B)^2 + 8J^2}}\right]}.$$

NON-CONSERVING MAGNETIZATION

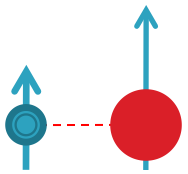

MIXED SPIN-(1/2,1) HEISENBERG DIMER

$$\langle\Psi_3|S_1^z|\Psi_3\rangle = -\frac{1}{2}\frac{J\Delta - 2D - 2g_-B}{\sqrt{(J\Delta - 2D - 2g_-B)^2 + 8J^2}},$$

$$\langle\Psi_3|\mu_2^z|\Psi_3\rangle = \frac{1}{2}\left[1 + \frac{J\Delta - 2D - 2g_-B}{\sqrt{(J\Delta - 2D - 2g_-B)^2 + 8J^2}}\right],$$

$$M = \langle\Psi_3|\left(g_1 S_1^z + g_2\mu_2^z\right)|\Psi_3\rangle$$

$$= \frac{g_2}{2} - \frac{g_-}{2}\frac{J\Delta - 2D - 2g_-B}{\sqrt{(J\Delta - 2D - 2g_-B)^2 + 8J^2}}.$$

$$\langle\Psi_5|S_1^z|\Psi_5\rangle = \frac{1}{2}\frac{J\Delta - 2D + 2g_-B}{\sqrt{(J\Delta - 2D + 2g_-B)^2 + 8J^2}},$$

$$\langle\Psi_5|\mu_2^z|\Psi_5\rangle = -\frac{1}{2}\left[1 + \frac{J\Delta - 2D + 2g_-B}{\sqrt{(J\Delta - 2D + 2g_-B)^2 + 8J^2}}\right]$$

$$M = \langle\Psi_5|\left(g_1 S_1^z + g_2\mu_2^z\right)|\Psi_5\rangle$$

$$= -\frac{g_2}{2} + \frac{g_-}{2}\frac{J\Delta - 2D - 2g_-B}{\sqrt{(J\Delta - 2D - 2g_-B)^2 + 8J^2}}.$$

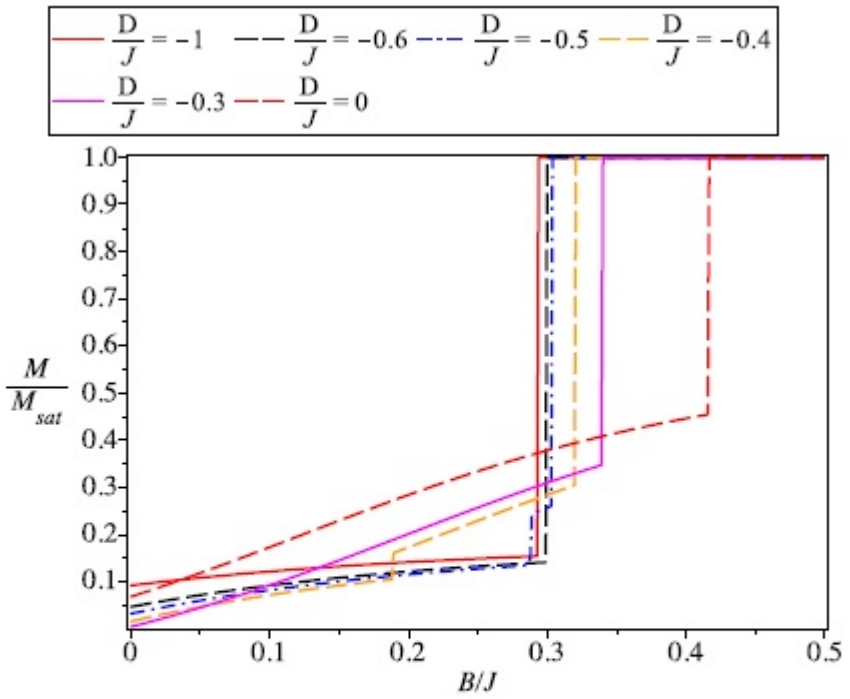

Zero-temperature normalized magnetization curves of the mixed spin-(1/2,1) dimer by assuming the isotropic Heisenberg coupling $\Delta = 1$, several values of the uniaxial single-ion anisotropy, and the Landé g factors $g_1 = 6$ and $g_2 = 2$. $M_{sat} = \frac{1}{2}(g_1 + 2g_2)$.

NON-CONSERVING MAGNETIZATION

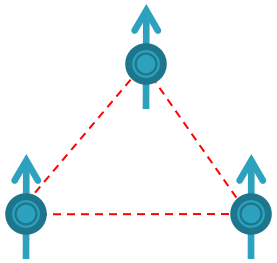

SPIN-1/2 HEISENBERG TRIMER

$$\mathcal{H}_{\rm trim} = J\left(S_1^x S_2^x + S_1^y S_2^y + \Delta S_1^z S_2^z + S_1^x S_3^x + S_1^y S_3^y + \Delta S_1^z S_3^z + S_2^x S_3^x + S_2^y S_3^y + \Delta S_2^z S_3^z\right) - g_1 B S_1^z - g_2 B\left(S_2^z + S_3^z\right)$$

$$\varepsilon_{1,2} = \frac{3J}{4} \mp \frac{1}{2}(g_1 + 2g_2)B,$$

$$\varepsilon_{3,4} = -\frac{J}{4}(2+\Delta) \mp \frac{1}{2} g_1 B,$$

$$\varepsilon_{5,6} = \frac{J}{4}(1-\Delta) \pm Q_+ + \frac{1}{2} g_2 B,$$

$$\varepsilon_{7,8} = \frac{J}{4}(1-\Delta) \pm Q_- - \frac{1}{2} g_2 B,$$

$$Q_\pm = \tfrac{1}{2}\sqrt{2J^2 + (J \pm g_- B)^2}.$$

$$|\Psi_1\rangle = |\uparrow\uparrow\uparrow\rangle, \quad |\Psi_2\rangle = |\downarrow\downarrow\downarrow\rangle,$$

$$|\Psi_3\rangle = |\uparrow\rangle_1 |S\rangle_{23}, \quad |\Psi_4\rangle = |\downarrow\rangle_1 |S\rangle_{23},$$

$$|\Psi_{5,6}\rangle = \frac{1}{\sqrt{2 + c_\pm^2}}\left(\sqrt{2}|\uparrow\rangle_1 |T_0\rangle_{23} + c_\pm |\downarrow\rangle_1 |T_+\rangle_{23}\right),$$

$$|\Psi_{7,8}\rangle = \frac{1}{\sqrt{2 + \bar{c}_\pm^2}}\left(\sqrt{2}|\downarrow\rangle_1 |T_0\rangle_{23} + \bar{c}_\pm |\uparrow\rangle_1 |T_-\rangle_{23}\right),$$

$$c_\pm = \frac{-J\Delta + 2g_- B \pm Q_+}{J\Delta},$$

$$\bar{c}_\pm = \frac{-J\Delta - 2g_- B \pm Q_-}{J\Delta}.$$

$$|S\rangle = \frac{1}{\sqrt{2}}(|\uparrow\downarrow\rangle - |\downarrow\uparrow\rangle), \quad |T_+\rangle = |\uparrow\uparrow\rangle,$$

$$|T_-\rangle = |\downarrow\downarrow\rangle, \quad |T_0\rangle = \frac{1}{\sqrt{2}}(|\uparrow\downarrow\rangle + |\downarrow\uparrow\rangle).$$

NON-CONSERVING MAGNETIZATION

SPIN-1/2 HEISENBERG TRIMER

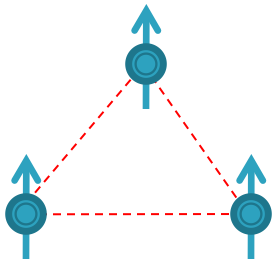

$$\langle\Psi_8|\{g_1 S_1^z + g_2(S_2^z + S_3^z)\}|\Psi_8\rangle = \frac{1}{2}\frac{2g_1 - (g_1 - 2g_2)\bar{c}_-^2}{2 + \bar{c}_-^2}.$$

$$B_c = J\frac{2g_+\Delta - g_1 + \sqrt{(2g_-\Delta - g_1)^2 + 8g_1g_2}}{4g_1g_2}.$$

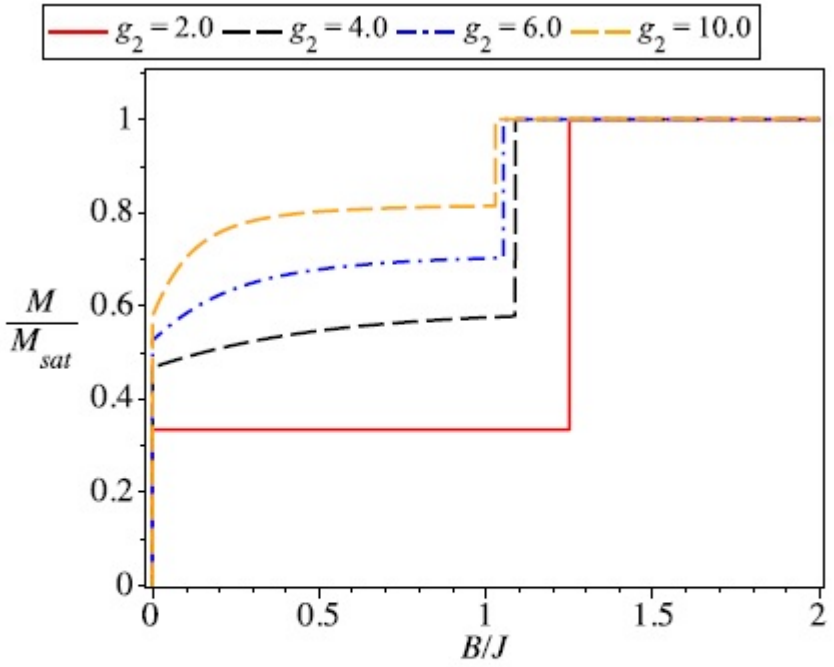

The zero-temperature normalized magnetization curves for the Heisenberg spin trimer with two different Landé g factors for $J = 1$, $\Delta = 2$, $g_1 = 2$, and $g_2 = 2$ (red, solid); $g_2 = 4$ (black, dashed); $g_2 = 6$ (blue, dot-dashed); and $g_2 = 10$ (orange, dashed). $M_{\text{sat}} = \frac{1}{2}(g_1 + 2g_2)$.

COORDINATION POLYMER $[\{(CuL)_2Dy\}\{Mo(CN)_8\}] \cdot 2CH_3CN \cdot H_2O$

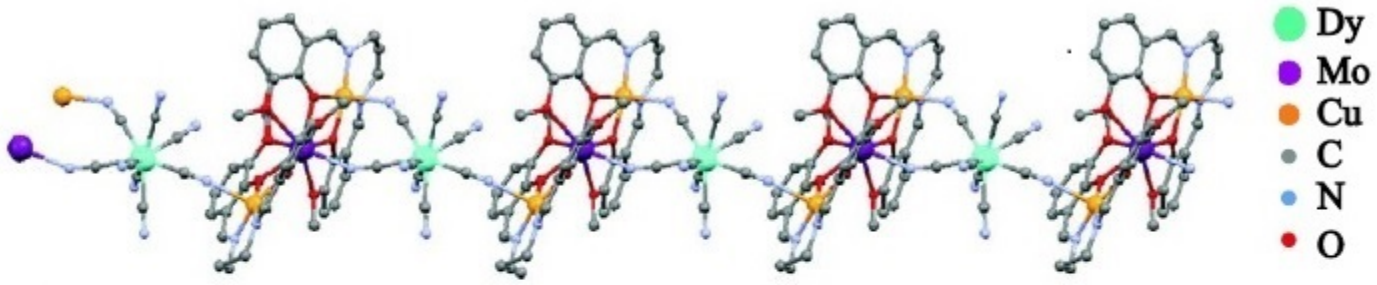

$[\{(CuL)_2Dy\}\{Mo(CN)_8\}] \cdot 2CH_3CN \cdot H_2O$

L^{2-}: N,N'-propylenebis(3- methoxysalicylideneiminato)

D. Visinescu, A. M. Madalan, M. Andruh, C. Duhayon, J.-P. Sutter, L. Ungur, W. Van den Heuvel and L. F. Chibotaru, Chem. Eur. J. **15**, 11808 (2009).

W. Van den Heuvel, L.F. Chibotaru, Phys. Rev. B **82**, 17 4436 (2010).

S. Bellucci, VO, O. Rojas, EPL **105**, 47012 (2014).

COORDINATION POLYMER $[\{(CuL)_2Dy\}\{Mo(CN)_8\}] \cdot 2CH_3CN \cdot H_2O$

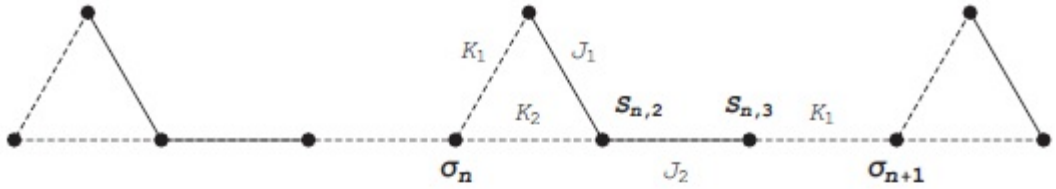

The magnetic structure of the single-chain magnet with Ising and Heisenberg bonds $[DyCuMoCu]_\infty$. The dashed lines denote Ising couplings while the solid lines correspond to the isotropic Heisenberg interactions. Spins $\mathbf{S}_{n,1}$ and $\mathbf{S}_{n,3}$ correspond to Cu^{2+} ions with $S = 1/2$ and isotropic (see footnote [1]) $g = 2.16$, $\mathbf{S}_{n,2}$ is the spin of the $S = 1/2$ Mo^{5+} ion with $g = 1.97$, the σ-spins correspond to the highly anisotropic Dy^{3+} ions with $g_z = 19.6$ and $g_x = g_y = 0$.

$$\mathcal{H} = \sum_{n=1}^{N} \left(\mathcal{H}_n - \mu_B g_3 \frac{B\cos\theta}{2} (\sigma_n + \sigma_{n+1}) \right),$$

$$\begin{aligned} \mathcal{H}_n = {} & J_1 \mathbf{S}_{n,1} \cdot \mathbf{S}_{n,2} + J_2 \mathbf{S}_{n,2} \cdot \mathbf{S}_{n,3} + K_2 S^z_{n,2} \sigma_n \\ & + K_1 \left(S^z_{n,1} \sigma_n + S^z_{n,3} \sigma_{n+1} \right) \\ & - \mu_B g_1 B \left(S^z_{n,1} + S^z_{n,3} \right) - \mu_B g_2 B S^z_{n,2}; \end{aligned}$$

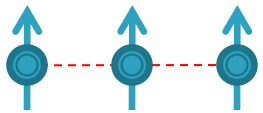

The structure of the block Hamiltonian

$$\begin{aligned} J_1 &= 8.3\ \mathrm{cm}^{-1} \\ J_2 &= -11.8\ \mathrm{cm}^{-1} \\ K_1 &= -15.3\ \mathrm{cm}^{-1} \\ K_2 &= 8\ \mathrm{cm}^{-1} \\ g_1 &= 2.16 \\ g_2 &= 1.97 \\ g_3 &= 19.6 \\ \mu_B &= 0.46686\ \mathrm{cm}^{-1}/\mathrm{T} \\ k_B &= 0.69504\ \mathrm{cm}^{-1}/\mathrm{K} \end{aligned}$$

COORDINATION POLYMER $[\{(CuL)_2Dy\}\{Mo(CN)_8\}] \cdot 2CH_3CN \cdot H_2O$

$$Z = \sum_{(\sigma)} \prod_{n=1}^{N} T_{\sigma_n,\sigma_{n+1}} = \mathrm{Tr}\, \mathbf{T}^N$$

$$T_{\sigma_n,\sigma_{n+1}} = e^{\frac{\beta\mu_B g_3 B\cos\theta}{2}(\sigma_n+\sigma_{n+1})} \mathrm{Tr}\, e^{-\beta\mathcal{H}_n}$$
$$= e^{\frac{\beta\mu_B g_3 B\cos\theta}{2}(\sigma_n+\sigma_{n+1})} \sum_{\text{eigenvalues}} e^{-\beta\varepsilon_j(\sigma_n,\sigma_{n+1})},$$

$$|3/2\rangle = |\uparrow\uparrow\uparrow\rangle$$
$$|-3/2\rangle = |\downarrow\downarrow\downarrow\rangle$$
$$|\pm 1/2; j\rangle = \frac{A_j^{\pm}|\uparrow\uparrow\downarrow\rangle + |\uparrow\downarrow\uparrow\rangle + B_j^{\pm}|\downarrow\uparrow\uparrow\rangle}{\sqrt{1+(A_j^{\pm})^2+(B_j^{\pm})^2}}$$

$$m^j_{\pm 1/2} = \pm\mu_B \frac{2g_1 + g_2\left\{(A_j^{\pm})^2+(B_j^{\pm})^2-1\right\}}{2\left\{(A_j^{\pm})^2+(B_j^{\pm})^2+1\right\}}$$

COORDINATION POLYMER $[\{(CuL)_2Dy\}\{Mo(CN)_8\}] \cdot 2CH_3CN \cdot H_2O$

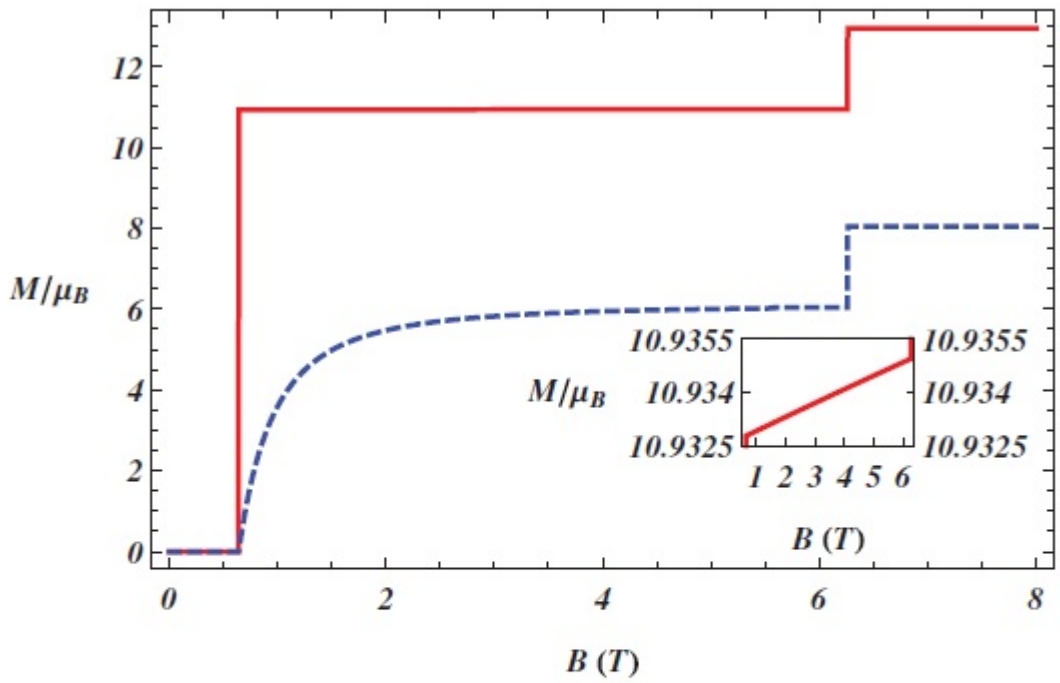

The plots of the magnetization processed $T = 0.00001$ K for the model of a single-crystal $[\mathrm{DyCuMoCu}]_\infty$, (solid red line) and powder sample (dashed blue line). The inset shows weak still monotonous growth of the magnetization at the broad quasi-plateau between $B_1 = 0.64093$ T with $M/\mu_B \approx 10.9325$ and $B_2 = 6.26021$ T with $M/\mu_B \approx 10.9350$.

COORDINATION POLYMER $[\{(CuL)_2Dy\}\{Mo(CN)_8\}] \cdot 2CH_3CN \cdot H_2O$

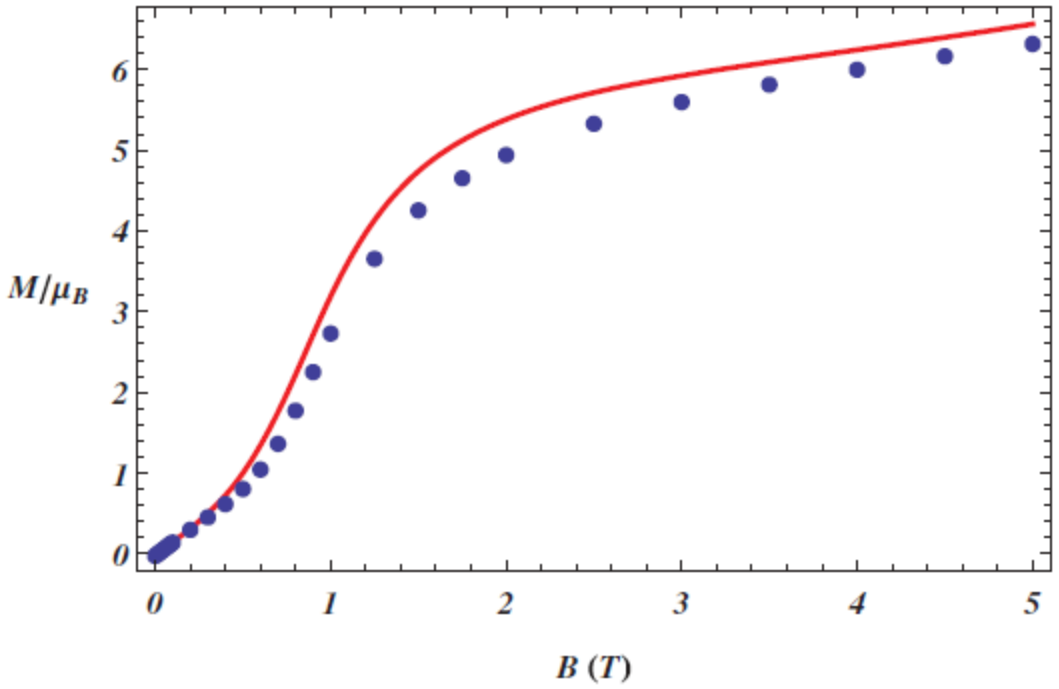

Fig. 3: (Color online) Powder magnetization of $[DyCuMoCu]_\infty$ at $T = 2\,K$ obtained by the angle integration of the theoretical curve (red solid line) and experimental points (see refs. [1,2]).

COORDINATION POLYMER $[\{(CuL)_2Dy\}\{Mo(CN)_8\}] \cdot 2CH_3CN \cdot H_2O$

$$|AF\rangle = \prod_{n=1}^{N/2} |\uparrow\rangle_{2n} |-1/2;1\rangle_{2n} |\downarrow\rangle_{2n+1} |1/2;1\rangle_{2n+1}.$$

$$|QP\rangle = \prod_{n=1}^{N} |\uparrow\rangle_n |1/2;1\rangle_n.$$

$$M_{AF} = \mu_B \frac{1}{2} (g_2 - 2g_1) \frac{(C_1^+)^2 - (C_1^-)^2}{C_1^+ C_1^-}$$

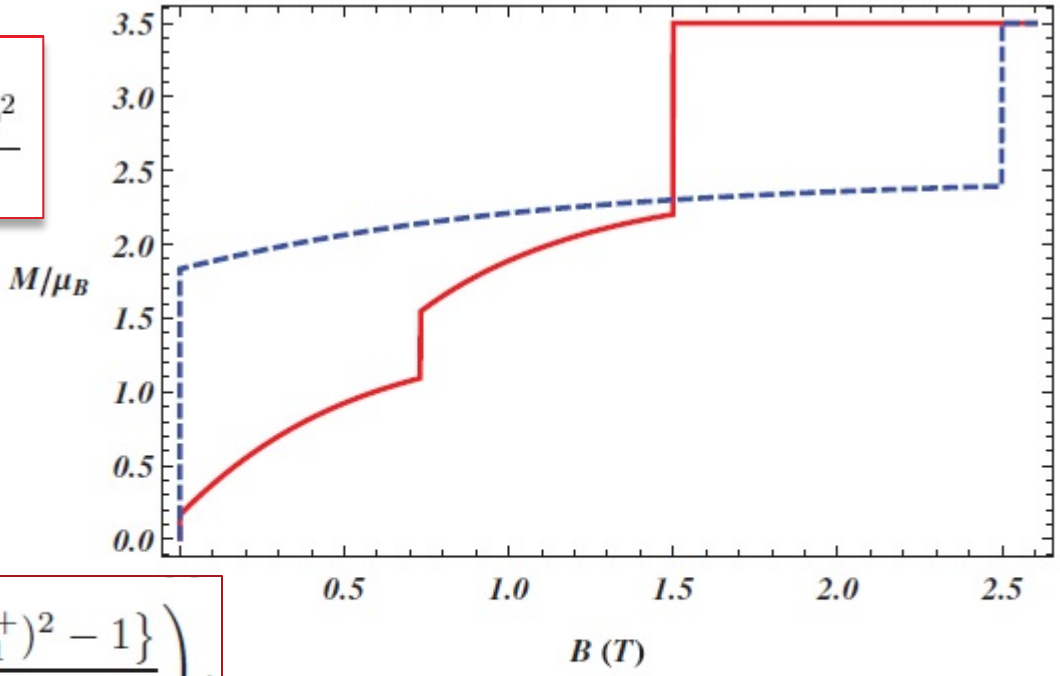

$$M_{QP} = \frac{\mu_B}{2} \left(g_3 + \frac{2g_1 + g_2 \{(A_1^+)^2 + (B_1^+)^2 - 1\}}{(A_1^+)^2 + (B_1^+)^2 + 1} \right).$$

Low-temperature magnetization curves for the isolated spin-(1/2) trimer with the structure of Cu-Mo-Cu part of the $[DyCuMoCu]_\infty$. The solid red line corresponds to $J_1 = J_2 = 1$, $g_1 = 1$, $g_2 = 5$; the dashed blue line corresponds to $J_1 = J_2 = 1$, $g_1 = 3$, $g_2 = 1$; $T = 0.00001$ K.

NEGATIVE G-FACTORS

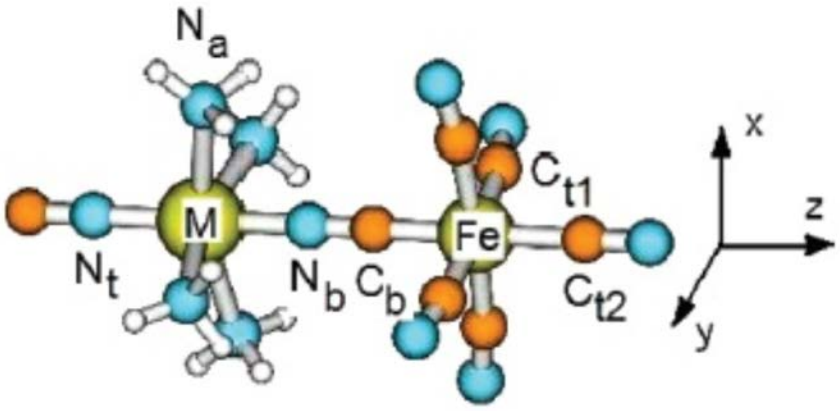

M=Cu, Ni

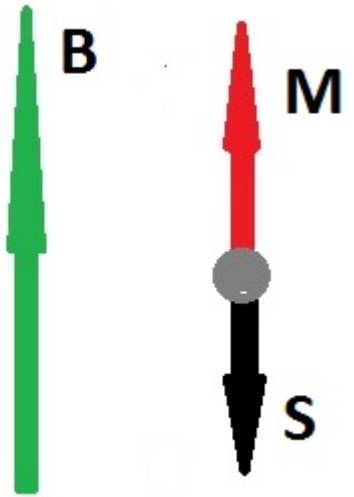

For Fe^{III}—CN—M^{II} (M=Cu, Ni)

$g_{Cu} \simeq 2.18$

$g_{Fe} \simeq -1.73$

M. Atanasov, P. Comba, C.A. Daul, Inorg. Chem. **47**, 2449 (2008).

NEGATIVE G-FACTORS

W.-G. Yin, X. Liu, A. M. Tsvelik, M. P. M. Dean, M. H. Upton, J. Kim, D. Casa, A. Said, T. Gog, T. F. Qi, G. Cao, and J. P. Hill, Phys. Rev. Lett. **111**, 057202 (2013).

X. Liu, V. M. Katukuri, L. Hozoi, W.-G. Yin, M. P. M. Dean, M. H. Upton, J. Kim, D. Casa, A. Said, T. Gog, T. F. Qi, G. Cao, A. M. Tsvelik, J. van den Brink, and J. P. Hill, Phys. Rev. Lett. **109**, 157401 (2012).

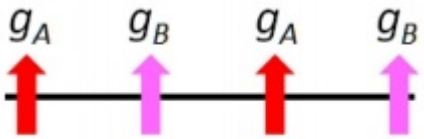

Sr_3CuIrO_6

$$g_{Cu} \simeq 2$$
$$g_{Ir} \simeq -3$$

W.-G. Yin, and C. R. Roth, A. M. Tsvelik, *Spin Frustration and a 'Half Fire, Half Ice' Critical Point from Nonuniform g-Factors*, arXiv:1510.00030, (2015).

ISING CHAIN WITH STAGGERED g-FACTORS WITH $g_A g_B < 0$

FM AND AM INTERACTION, FRUSTRATION, GEOMETRY OF BONDS

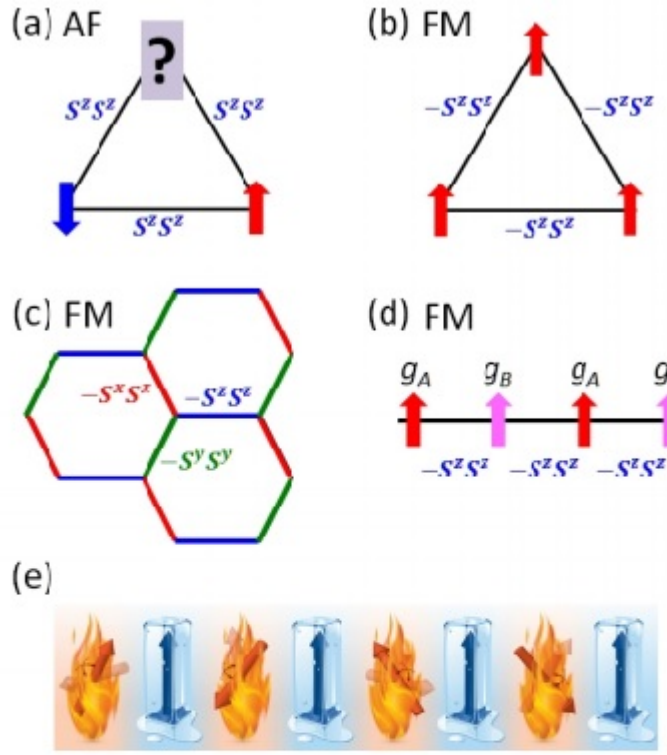

FIG. 1. (a) Frustrated spins on triangular lattice with AF interactions. (b) Unfrustrated spins for FM interactions. (c) Frustrated spins on honeycomb lattice with FM interactions whose anisotropic axes are bond dependent [12, 13]. (d) Spins in a chain with uniform FM interactions and alternating g-factors ($-g_B > g_A > 0$) are found frustrated. (e) A cartoon illustration of the 'half-fire, half-ice' critical point at which the spins on one sublattice are fully disordered and on the other are fully ordered.

ISING CHAIN WITH STAGGERED g-FACTORS WITH $g_A g_B < 0$

$$\mathcal{H}_{Is}^{1d} = J\sum_{j=1}^{N}\sigma_j\sigma_{j+1} - B\sum_{j=1}^{N/2}\left(g_A\sigma_{2j-1} + g_B\sigma_{2j}\right),$$

$$g_A > 0, \quad g_B < 0, \qquad |g_B| > g_A$$

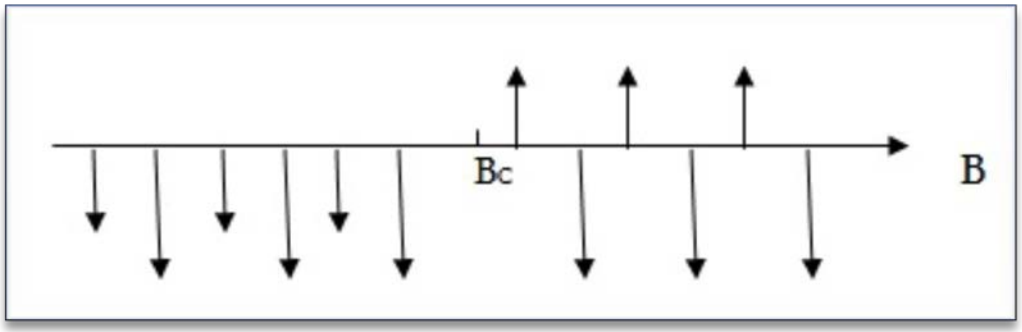

$$B_c = \frac{|J|}{g_A},$$

$$S/N = \log 2$$

$$\chi(0,T) = \frac{1}{16T}\left(e^{-\frac{J}{2T}}(g_A+g_B)^2 + e^{\frac{J}{2T}}(g_A-g_B)^2\right)$$

W.-G. Yin, and C. R. Roth, A. M. Tsvelik, *Spin Frustration and a 'Half Fire, Half Ice' Critical Point from Nonuniform g-Factors*, arXiv:1510.00030, (2015).

$$\mathcal{H}_{Is}^{AB} = J \sum_{i\in A, j\in B} \sigma_i \sigma_j - B \left(g_A \sum_{i\in A} \sigma_i + g_B \sum_{j\in B} \sigma_j \right).$$

$$g_A > 0, \quad g_B < 0, \qquad |g_B| > g_A$$

$$B_c = \frac{|J|d}{2g_A},$$

ISING DIAMOND CHAIN WITH INHOMOGENEOUS g-FACTORS

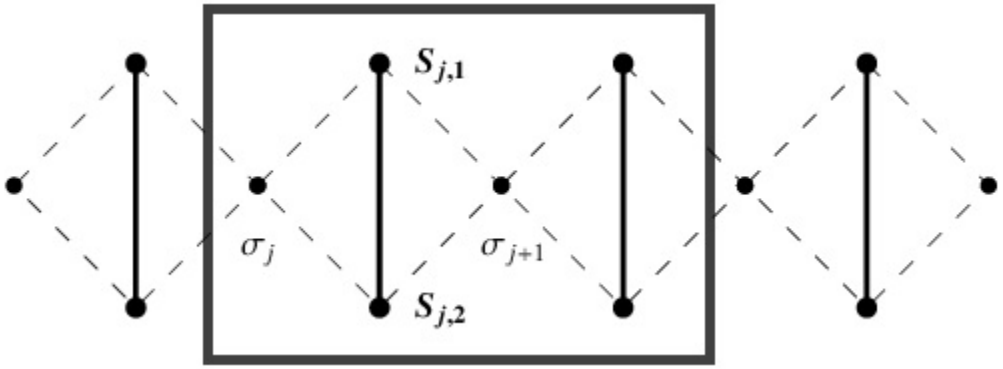

$$\mathcal{H}_I = \sum_{j=1}^{N} \left\{ \Delta S_{j,1}^z S_{j,2}^z + K(S_{j,1}^z + S_{j,2}^z)(\sigma_j + \sigma_{j+1}) - B(g_1 S_{j,1}^z + g_2 S_{j,2}^z) \right\} - B \sum_{j=1}^{N/2} (g_3 \sigma_{2j-1} + g_4 \sigma_{2j})$$

$$E_F^- = -\frac{n}{4}K + \frac{B}{2}\left(\sum g_{pos} - \sum |g_{neg}|\right),$$
$$E_F^+ = -\frac{n}{4}K - \frac{B}{2}\left(\sum g_{pos} - \sum |g_{neg}|\right),$$
$$E_S = -\frac{m}{4}K - \frac{B}{2}\left(\sum g_{pos} + \sum |g_{neg}|\right),$$

$$B_c = \frac{(n-m)K}{4\sum g_{pos}}.$$

$$\sum |g_{neg}| > \sum g_{pos}$$

$$B_c = \frac{(m-n)K}{4\sum |g_{neg}|},$$

$$\sum |g_{neg}| < \sum g_{pos}$$

ISING DIAMOND CHAIN WITH INHOMOGENEOUS g-FACTORS

Thus, having q spins with negative g-factors in the p-spin magnetic unit cell can lead to the interface with either q disordered spins or $p-q$ disordered spins in the unit cell depending on the relation between total negative and positive g-factors.

- one frustrated spin (1/6-fire-5/6-ice) $\quad g_3 < 0, \quad |g_3| < 2(g_1+g_2)+g_4, \quad B_c = \frac{2K}{g_3}$
- two frustrated spins (1/3-fire-2/3-ice) $\quad g_3 < 0,\ g_4 < 0, \quad |g_3+g_4| < 2(g_1+g_2), \quad B_c = \frac{4K}{g_3+g_4}$
  - $|g_3+g_4| > 2(g_1+g_2), \quad B_c = \frac{2|K|}{g_1+g_2}$
  - $\Delta > 0, \quad \Delta > |K|, \quad B_c = \frac{\Delta+2|K|}{2g_2}$
- three frustrated spins (1/2-fire-1/2-ice) $\quad g_1 < 0,\ g_3 < 0, \quad |2g_1+g_3| > 2g_2+g_4, \quad B_c = \frac{\Delta+2K}{2g_1+g_3}$
- four frustrated spins (2/3-fire-1/3-ice) $\quad g_3 < 0,\ g_4 < 0, \quad |g_3+g_4| > 2(g_1+g_2), \quad B_c = \frac{2|K|}{g_1+g_2}$
- five frustrated spins (1/6-fire-5/6-ice) $\quad g_3 < 0, \quad |g_3| > 2(g_1+g_2)+g_4, \quad B_c = \frac{2|K|}{g_4-2(g_1+g_2)}$

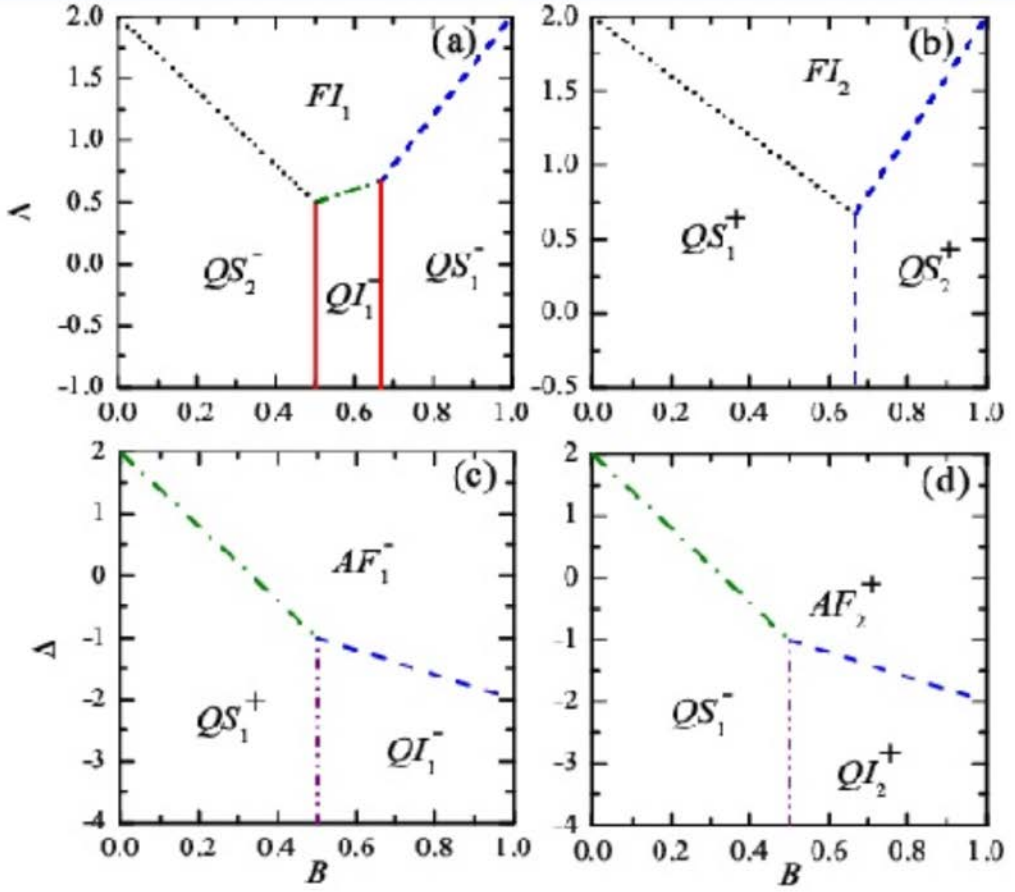

Figure 2: Zero temperature phase diagram Δ against B. (a) For $K = -1$, $g_1 = -2$, $g_2 = -2$, $g_3 = 4$ and $g_4 = 3$. (b) For $K = -1$, $g_1 = 2$, $g_2 = 2$, $g_3 = -3$ and $g_4 = -3$. (c) For $K = -1$, $g_1 = -2$, $g_2 = 1$, $g_3 = 4$ and $g_4 = -2$. (d) $K = 1$, $g_1 = 2$, $g_2 = -1$, $g_3 = -2$ and $g_4 = 4$.

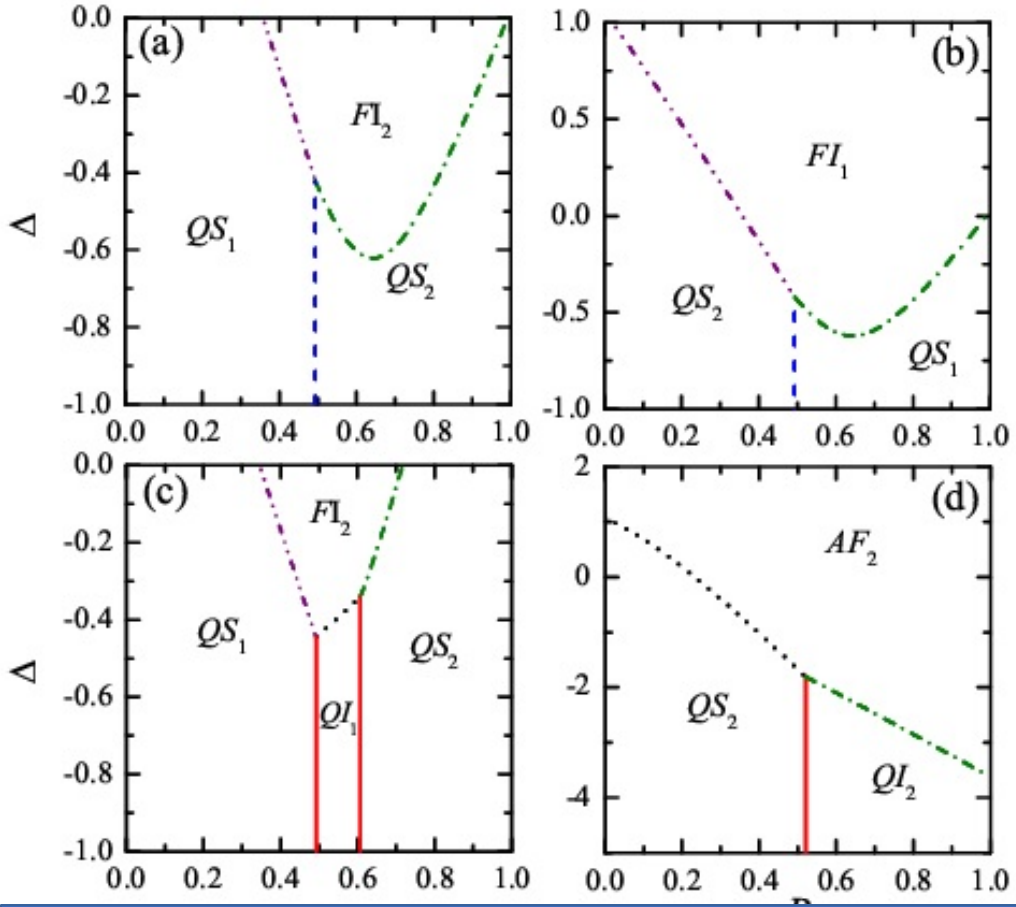

Figure 3: Zero temperature phase diagrams for the Ising-Heisenberg diamond chain at fixed $J = 1$ and $\gamma = 0.5$. (a) For $K = -1$, $g_1 = 2$, $g_2 = 1.2$, $g_3 = -3$ and $g_4 = -3$. (b) For $K = 1$, $g_1 = 2$, $g_2 = 1.2$, $g_3 = 3$ and $g_4 = 3$. (c) For $K = -1$, $g_1 = 2$, $g_2 = 2$, $g_3 = -3$ and $g_4 = -4$. (d) For $K = -1$, $g_1 = -2$, $g_2 = 2$, $g_3 = -4$ and $g_4 = 3$.

$$B_c = \sqrt{\frac{16K^2}{(g_3+g_4)^2} + \frac{4J^2\gamma^2}{(g_3+g_4)^2 - 4(g_1+g_2)^2}}.$$

1/3-fire-2/3-ice

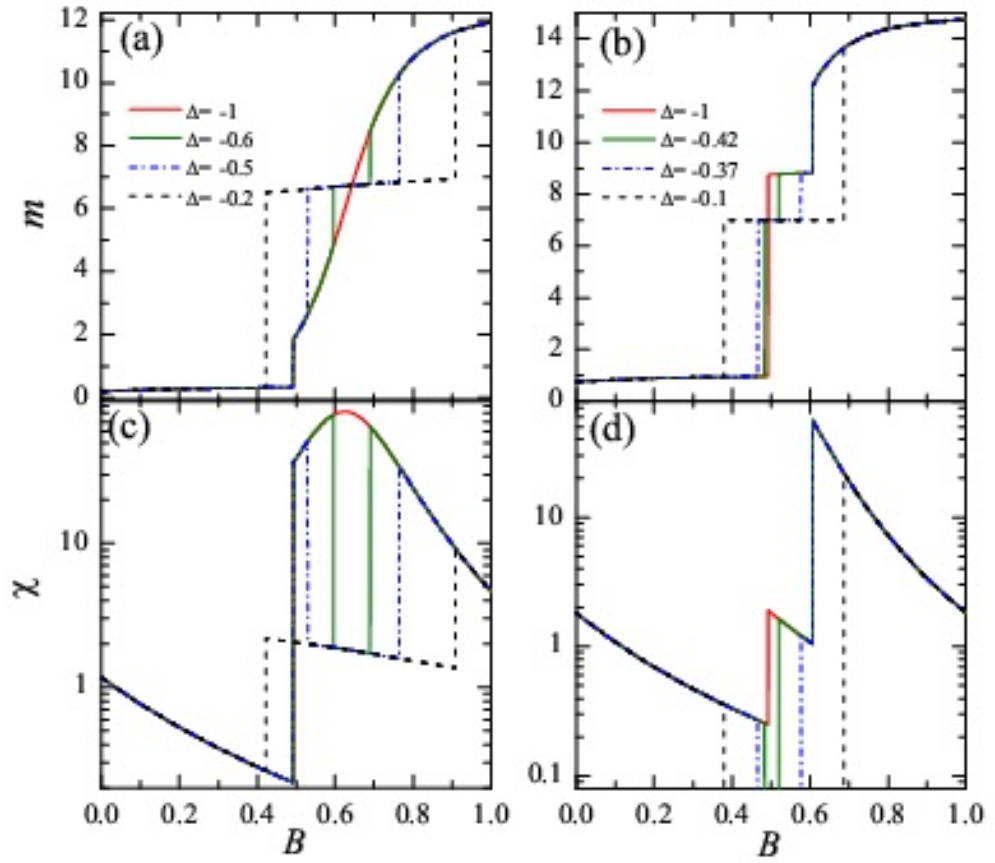

Figure 4: Zero temperature magnetization (magnetic susceptibility) as a function of magnetic field B for $J = 1$, $K = -1$ and $\gamma = 0.5$. Left panel, (a) and (c), $g_1 = 2$, $g_2 = 1.2$, $g_3 = -3$ and $g_4 = -3$; roght panel, (b) and (d), For $g_1 = 2$, $g_2 = 2$, $g_3 = -3$ and $g_4 = -4$.

Dynamic properties of $g_1 - g_2$ XY chain

$$\mathcal{H}_0 = J\sum_{l=1}^{N}(s_l^x s_{l+1}^x + s_l^y s_{l+1}^y) - h\mu\sum_{l=1}^{N/2}(g_1 s_{2l-1}^z + g_2 s_{2l}^z).$$

$$\mathcal{H}_0 = \frac{J}{2}\sum_{j=1}^{N}\left(c_j^\dagger c_{j+1} - c_j c_{j+1}^\dagger\right) - \sum_{j=1}^{N/2}\left(h_1 c_{2j-1}^\dagger c_{2j-1} + h_2 c_{2j}^\dagger c_{2j}\right) + h_+\frac{N}{2}$$

$$h_+ \equiv \frac{h_1 + h_2}{2}, \quad \delta \equiv \frac{h_1 - h_2}{2}, \quad h_j \equiv \mu g_j h$$

$$c_j = \frac{1}{\sqrt{N}}\sum_k e^{-ikj} c_k, \quad k = \frac{2\pi l}{\pi}, \quad l = 0, \ldots, N-1$$

$$\mathcal{H}_0 = \sum_k \left(J\cos k - h_+\right) c_k^\dagger c_k + \delta\sum_k\left(c_k^\dagger c_{k+\pi} + c_{k+\pi}^\dagger c_k\right) + h_+\frac{N}{2}$$

$$\mathcal{H}_0 = \sum_k \left(J\cos k - h_+\right) c_k^\dagger c_k + \delta \sum_k \left(c_k^\dagger c_{k+\pi} + c_{k+\pi}^\dagger c_k\right) + h_+ \frac{N}{2}$$

$$a_k = u_k c_k + v_k c_{k+\pi}, \quad c_k = u_k a_k - v_k a_{k+\pi}$$

$$u_k \equiv \frac{\mathrm{sgn}(\delta)}{\sqrt{2}} \sqrt{1 + \frac{|J\cos k|}{\sqrt{J^2\cos^2 k + \delta^2}}}, \quad v_k \equiv \frac{\mathrm{sgn}(J\cos k)}{\sqrt{2}} \sqrt{1 - \frac{|J\cos k|}{\sqrt{J^2\cos^2 k + \delta^2}}}$$

$$\mathcal{H}_0 = \sum_k \Lambda_k a_k^\dagger a_k + h_+ \frac{N}{2}$$

$$\Lambda_k \equiv -h_+ + \mathrm{sgn}(J\cos k)\sqrt{J^2\cos^2 k + \delta^2}$$

$$T = 0, \quad g_1 g_2 < 0$$

$$\mathcal{E} = -\frac{1}{\pi}\sqrt{J^2+\delta^2}\mathrm{E}(\kappa)$$

$$\kappa = \frac{|J|}{\sqrt{J^2+\delta^2}}$$

$$m_z = \frac{1}{4\pi}\frac{(g_1-g_2)^2}{\sqrt{J^2+\delta^2}}h\mathrm{K}(\kappa)$$

$$m_z \approx \frac{(g_1-g_2)^2}{8\sqrt{J^2+\delta^2}}h, |h| \to \infty, \quad m_z \approx \frac{1}{4\pi}\frac{(g_1-g_2)^2}{\sqrt{J^2+\delta^2}}h\ln\frac{4\sqrt{J^2+\delta^2}}{|\delta|}, |h| \to 0$$

$$\chi_z = \frac{1}{4\pi}\frac{(g_1-g_2)^2}{\sqrt{J^2+\delta^2}}\left[\mathrm{K}(\kappa)-\mathrm{E}(\kappa)\right]$$

$$\chi_z \approx \frac{(g_1-g_2)^2}{16}\frac{J^2}{(J^2+\delta^2)^{3/2}}, |h| \to \infty, \quad \chi_z \approx \frac{1}{4\pi}\frac{(g_1-g_2)^2}{\sqrt{J^2+\delta^2}}\left[\ln\frac{4\sqrt{J^2+\delta^2}}{|\delta|}-1\right], |h| \to 0$$

$$g_1 g_2 > 0, \quad \langle s_1^z \rangle = \frac{k_0}{\pi} - \frac{1}{2} + \frac{\delta}{\pi\sqrt{J^2+\delta^2}} \mathrm{F}(\varphi_0|\kappa), \quad \langle s_2^z \rangle = \frac{k_0}{\pi} - \frac{1}{2} - \frac{\delta}{\pi\sqrt{J^2+\delta^2}} \mathrm{F}(\varphi_0|\kappa)$$

$$g_1 g_2 < 0, \quad \langle s_1^z \rangle = \frac{\delta}{\pi\sqrt{J^2+\delta^2}} \mathrm{K}(\kappa), \quad \langle s_2^z \rangle = -\frac{\delta}{\pi\sqrt{J^2+\delta^2}} \mathrm{K}(\kappa) = -\langle s_1^z \rangle$$

$$S_{\alpha\alpha}(q,\omega) \equiv \frac{1}{N} \sum_{j=1}^{N} \sum_{n=1}^{N} e^{iqn} \int_{-\infty}^{\infty} dt e^{i\omega t} \langle s_j^\alpha(t) s_{j+n}^\alpha \rangle g_j g_{j+n}$$

O.Derzhko,T.Krokhmalskii,J.Stolze "Dynamic properties of the dimerized spin-1/2 isotropic XY chain in a transverse field ", J.Phys.A:Math.Gen. **35** (2002) 3573-3596.

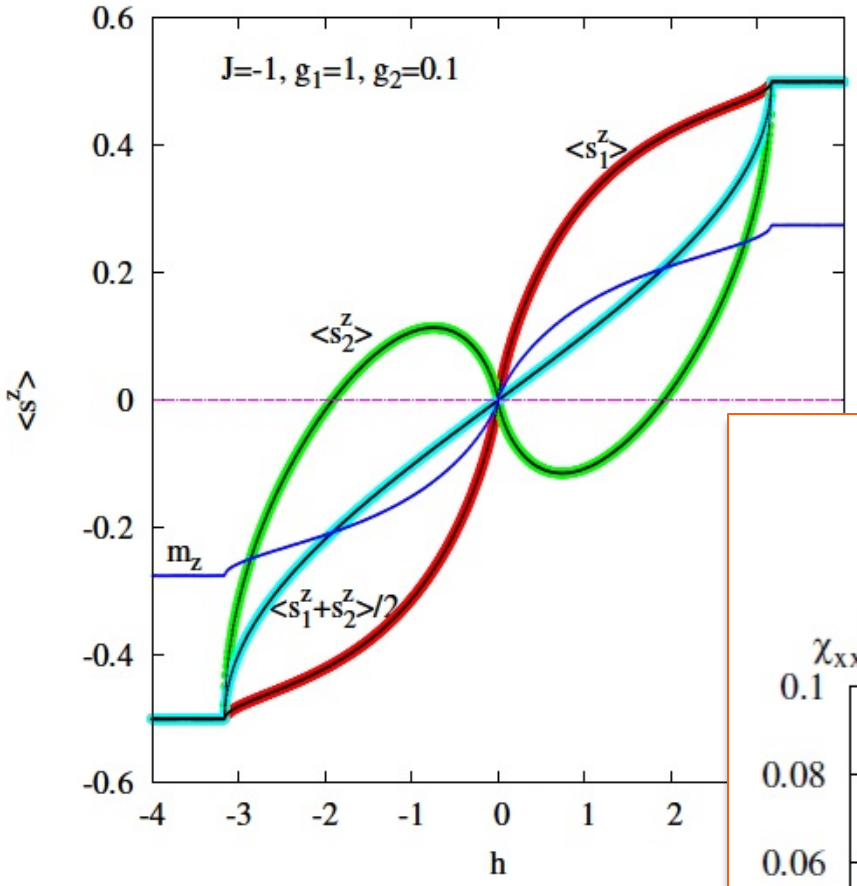
J=-1, g1=1, g2=0.1
<s1z>
<s2z>
mz
<s1z+s2z>/2
<sz>
h
0.6
0.4
0.2
0
-0.2
-0.4
-0.6
-4
-3
-2
-1
0
1
2

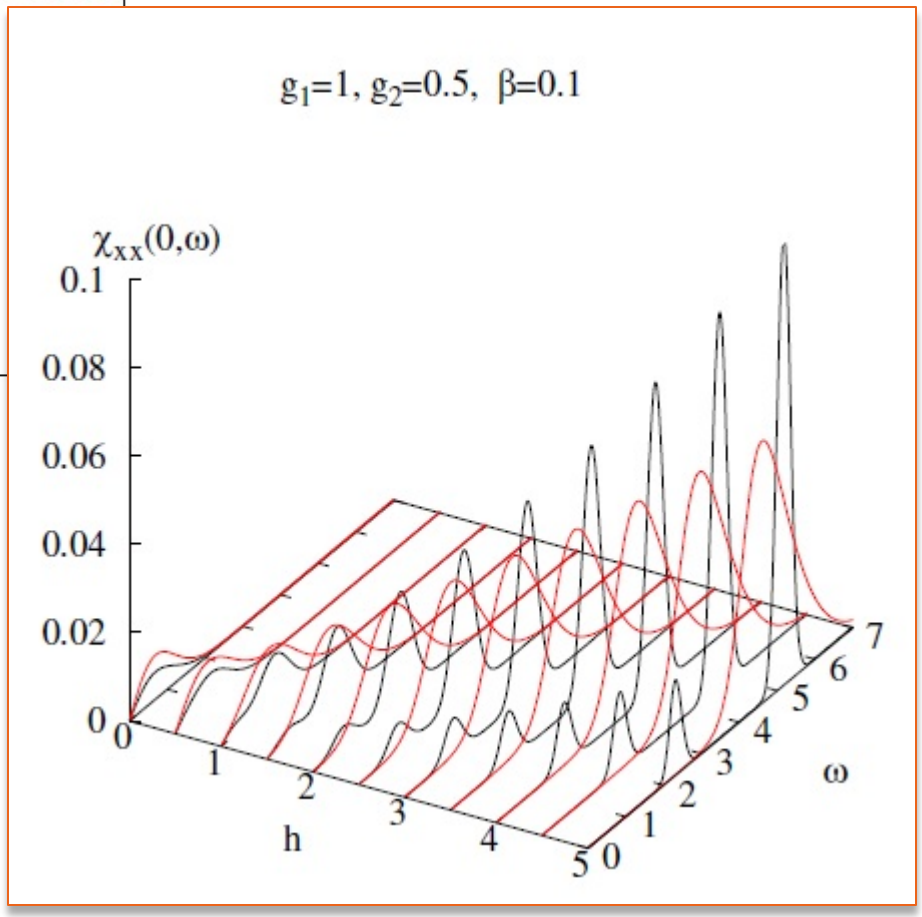
g1=1, g2=0.5, β=0.1
χxx(0,ω)
0.1
0.08
0.06
0.04
0.02
0
h
ω
0
1
2
3
4
5
6
7

V. CONCLUSION

- Non-conserving magnetization alters the magneto-thermal properties of magnetic system quite seriously
- Different g-factors – simplest way to get the non-conserving magnetization
- For finite spin system it leads to:
  - non-linear magnetic field dependence of the energy levels
  - non-constant magnetization within one eigenstate
  - non-plateau form of the magnetization curve, which mimics the magnetization curve for many-body systems with the bands of magnetic excitations
- the g-factors of different signs within one systems can lead to the novel frustration for ferromagnetic systems
- many interfaces with various ordered and disordered sublattices are possible for the Ising models with g-factors of different signs
- for the XX-chain staggered g-factors lead to novel $T = 0$ behavior of magnetization and susceptibility
- the dynamical structure factors are also affected by the difference of g-factros

Thank you for attention !